



ABSTRACT

Electronic shifters (E-shifter) determine the operating modes of a vehicle and therefore require robust redundancy built into them to make sure critical function is maintained despite whatever glitches can occur. For that redundancy, many manufacturers design with identical independent sensing devices. This document details how the [TMAG5170D](#), which has two independent sensing devices integrated into a single package, can be used to design an E-shifter.

Table of Contents

1 Introduction	2
2 Choosing a Mechanical Implementation	3
3 Choosing a Magnetic Implementation	4
4 Magnet Sensor Placement	6
5 Prototyping and Bench Testing	8
6 Error Sources	12
7 Summary	13
8 References	14

Trademarks

All trademarks are the property of their respective owners.

1 Introduction

End users typically expect E-shifters to be robust, tactile, and requiring minimal dexterity to operate. From a contract automanufacturers perspective, the design needs to satisfy functional safety requirements and the underlying design needs to be flexible and precise enough to be possibly packaged up and reused in several different car models. After satisfying these fundamental objectives, there is the desire to minimize cost, power, and design size.

This document shows a design process for a possible version of the E-shifter with the [TMAG5170D](#), a multi-sensor device designed specifically for the redundancy desired in systems requiring functional safety. The featured stacked die in the package reducing the spacing between sensing elements reduces the error between sensors. Additionally, the lower wake-up and sleep modes provide the E-shifter designer some opportunity to minimize power consumption.

Figure 1-1 summarizes the design flow presented in this document.

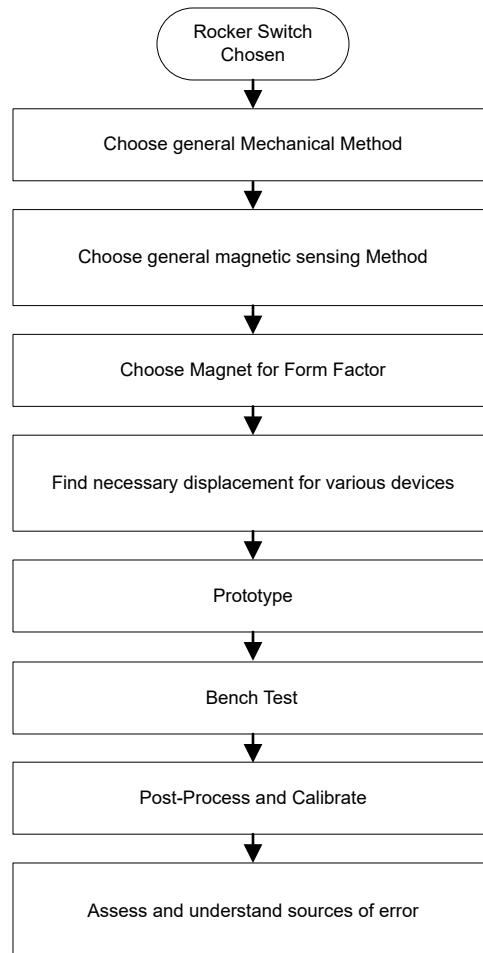


Figure 1-1. Development Flow

2 Choosing a Mechanical Implementation

The mechanical implementation of the Eshifter not only has influence over the end user's experience, but also has influence on what magnet-sensor pairings are viable. In [Figure 2-1](#) there are three possible mechanical implementations. The left is a dial, the middle a joystick, and the right is lever. This document examines the lever design.

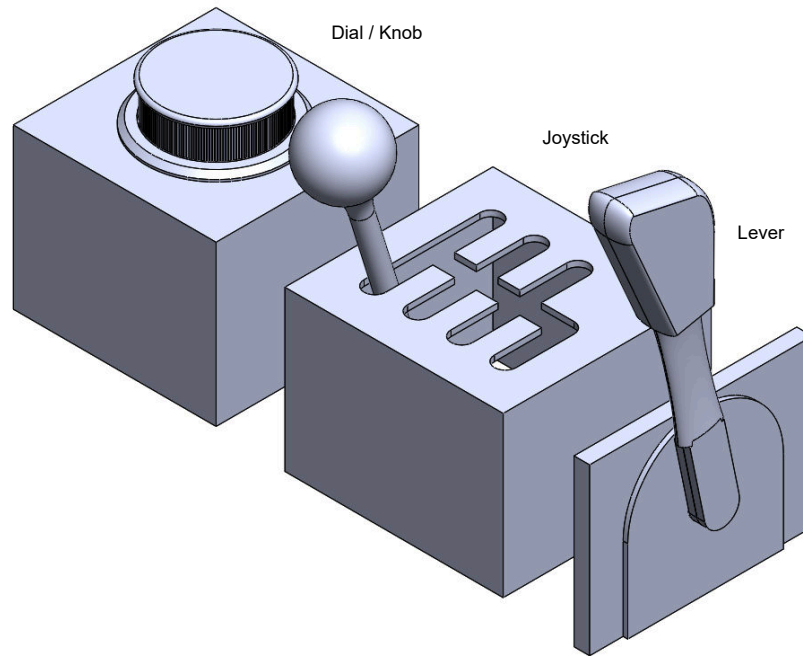


Figure 2-1. Eshifter Mechanical Implementation

3 Choosing a Magnetic Implementation

For many designs the most logical place for the magnet is in the moving component that we desire to sense, rather than the sensor which is likely powered through traces and wires routed from some far-off supply. As such, the magnet needs to fit somewhere in the shifter lever and depending on where the magnet is placed, different kinds of magnets can be appropriate. Figure 3-1 shows two possible magnet implementations. On the left is a diametric magnet centered at the fulcrum of the lever, while on the right is an axial magnet situated some distance from the rotation axis.

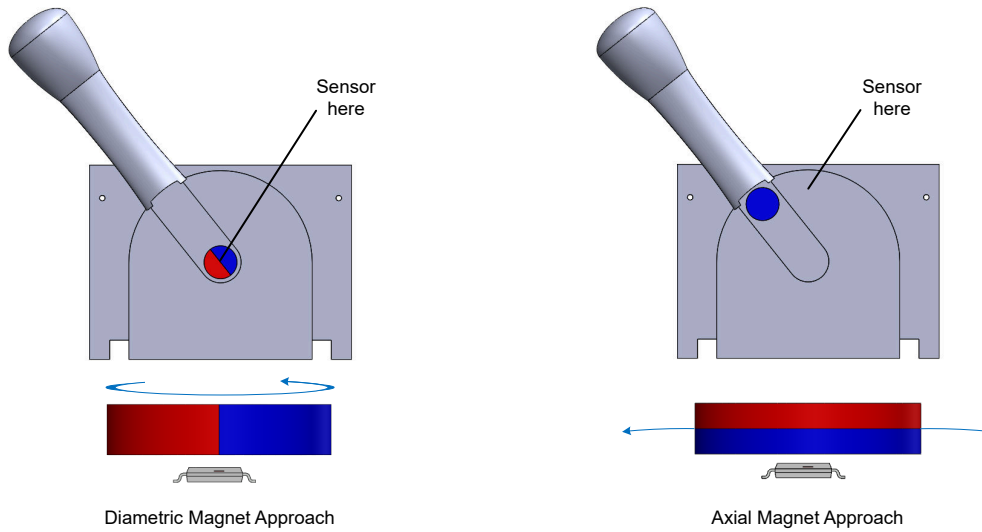


Figure 3-1. Magnetic Implementation

The goal of the design presented in this application report is to have an output that is linear without aliasing such as the desired signal shown in Figure 3-2. For detecting objects that rotate around an axis, 3d or multi-axis sensing devices are more suitable than single axis sensing devices. Not only do multi-axis sensing devices have flexibility of package orientation, but are also immune to aliasing that is otherwise unavoidable with a single axis sensing device. This is due to the fact that fields perpendicular to each other exhibit behavior analogous to sine and cosine waves. By taking the arctan of two perpendicular fields, a linear output over a wide range of motion of the magnet can be derived.

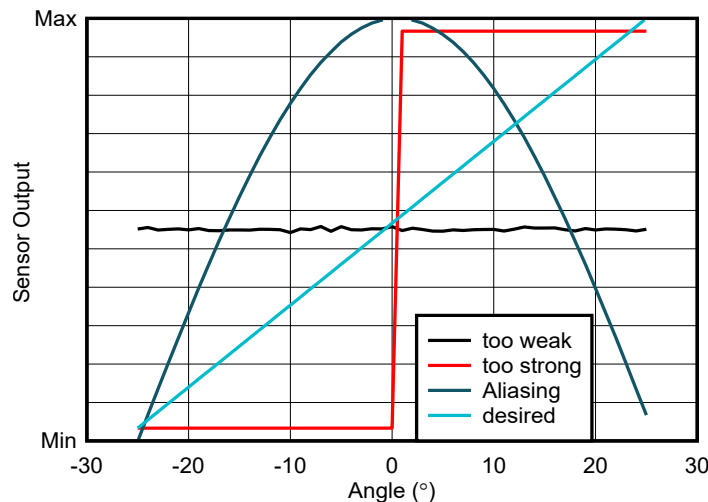


Figure 3-2. Output Plots

For the diametric magnet, field behavior like in [Figure 3-3](#) is expected while for the axial magnet field behavior like in [Figure 3-4](#) is expected.

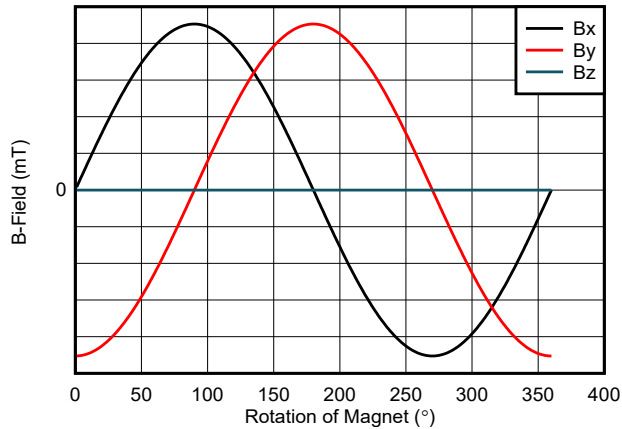


Figure 3-3. B-Field Behavior for Diametric Approach

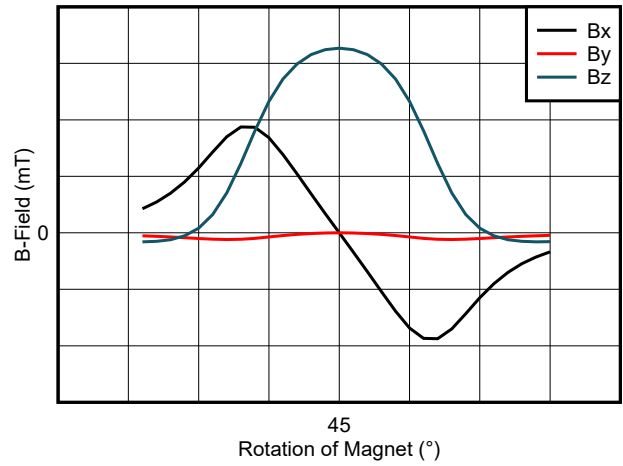


Figure 3-4. B-Field Behavior For Axial Approach

Due to the shifter in this design rotating and requiring redundant measurement, the TMAG5170D is selected.

4 Magnet Sensor Placement

For the designs presented in this application report, aside from the enclosure that houses the shifter sensing system, there are two constraints that dictate the relative placement between magnet and sensor. These constraints are the device noise floor and the max sensing range. The goal is to get the largest field detected by the device to be a little less than the max sensing value for optimizing the signal to noise ratio. However, that can be impossible, so quantifying the error associated with different peak field strengths can be useful for gauging whether the magnet is close enough or strong enough for the desired mechanical-magnetic implementation. For the diametric approach where the peak Bx and By fields are expected to be nearly equal, [Figure 4-1](#) shows an estimation of what the max error can be for 1 sigma magnetic noise of 185µT. [Figure 4-1](#) and all subsequent plots in this section were extrapolated from simulations done in [Texas Instruments Magnetic Sense Simulator \(TIMSS\)](#).

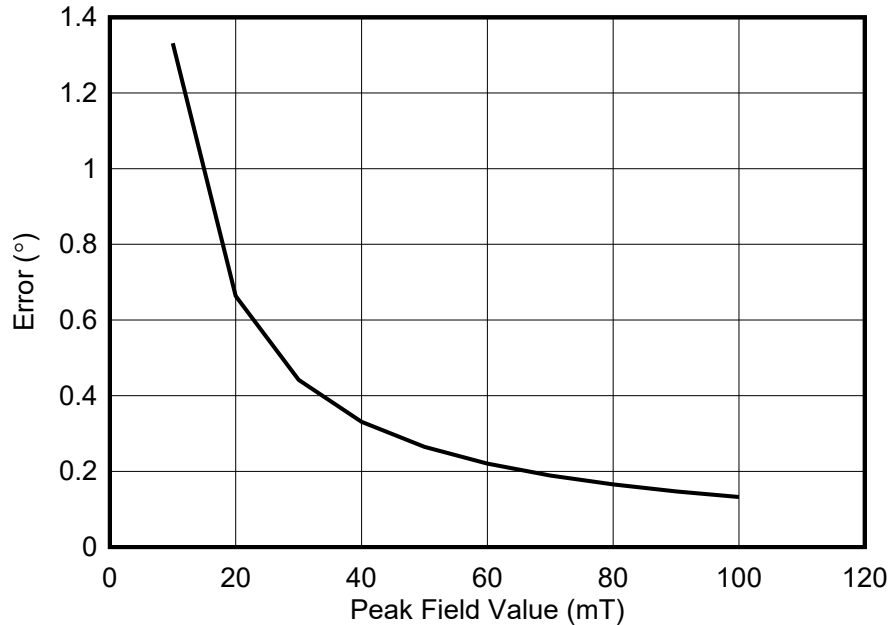


Figure 4-1. Error Vs. Peak Field Strength for Diametric Approach

With the results observed in [Figure 4-1](#), there is some guidance for determining what size and grade of magnet as well as what reasonable distance or air gap can be between magnet and the device. For gauging the impact of the distance between the magnet and device denoted by "air-gap" in [Figure 4-2](#), [Figure 4-3](#) shows an N42, 12.7mm diameter, 3.175mm thick the peak field values measured by the TMAG5170 for any z-offset from the magnet origin within -8mm and -2.5mm.

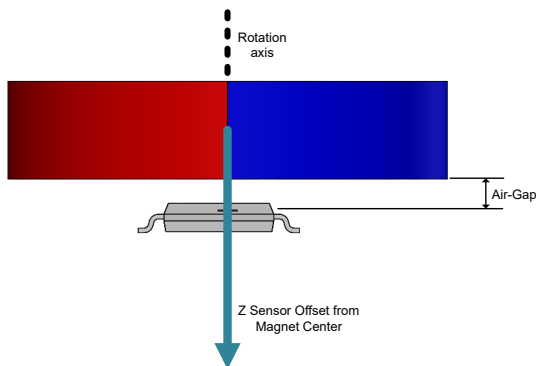


Figure 4-2. Sensor Z-offset Sweep Diagram

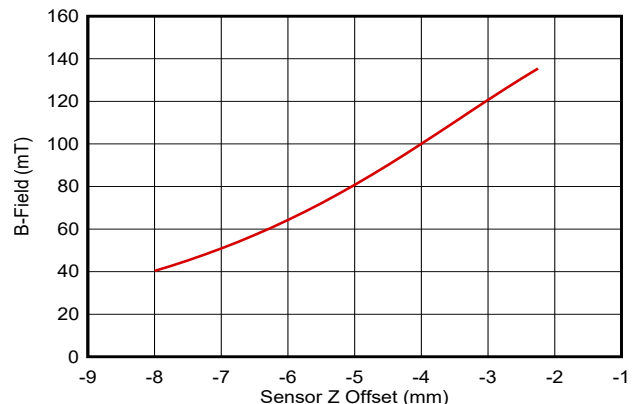


Figure 4-3. Max Bx or By Field Versus Sensor Z offset

For gauging the impact of magnet size, [Figure 4-4](#) shows what kind of field values can be observed for an N42, 3.175mm thick, with diameters ranging from 2mm to 20mm with an air gap of 7mm from the sensor.

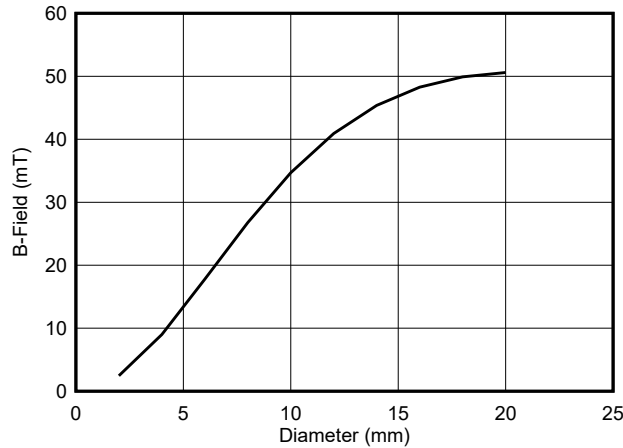


Figure 4-4. Max Bx or By Field Versus Magnet Diameter

From [Figure 4-1](#) a minimum of about 15mT is needed to have an error of 1° or less per the device noise floor. [Figure 4-3](#) shows that for larger air-gaps between the magnet and device, the expected signal amplitude decreases; however, for the magnet size chosen in the placement region of interest the amplitude appears to have at least roughly double the what is required for error under 1°. Lastly, [Figure 4-4](#) shows that for the desired offset of 7mm, a magnet with as small as a 5.4mm diameter can potentially be used for 1° error if only considering error from noise.

As noise is not the only source of error, some analysis with sweeping offsets per manufacturing and assembly tolerances is recommended. [Figure 4-5](#) indicates that smaller diameters are less forgiving in error for the same offset. Based on a large group of simulation data not shown, offsets less than 10% of the magnet diameter length frequently appear to provide less than 1° error. As for magnet thickness, [Figure 4-6](#) suggests that only a slight change in angle error is observed for different thicknesses.

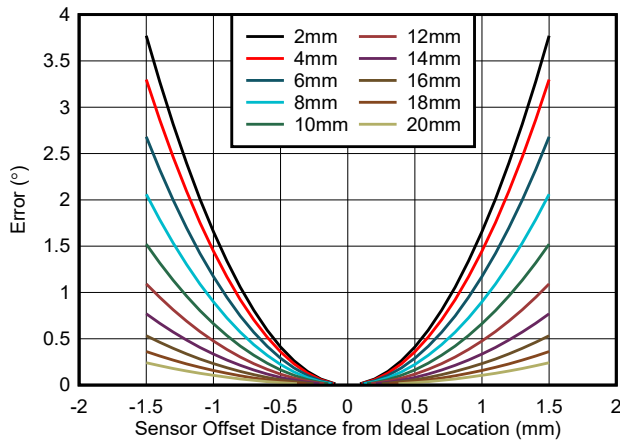


Figure 4-5. Diameter Sweep

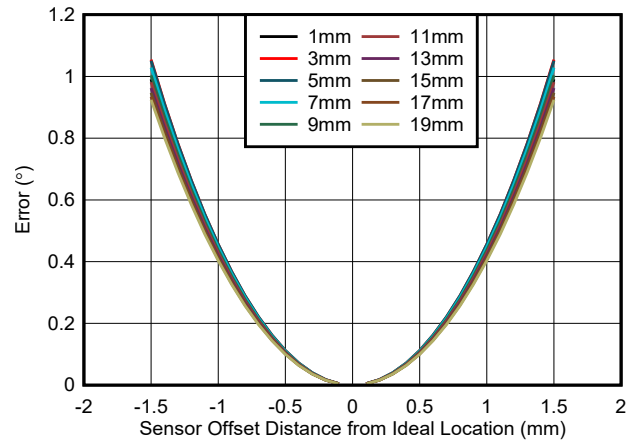


Figure 4-6. Thickness Sweep

5 Prototyping and Bench Testing

While simulation can be helpful for the preliminary design and assessing feasibility, prototyping and bench testing is necessary for verifying actual performance. Simulation excludes unrealized variables and therefore does not have all the necessary parameters to exactly match real-world test cases. Bench tests reveal some of the possible discrepancies between simulations and a fabricated system with manufacturing and assembly tolerances.

The fabricated diametric design presented in this application note is shown in [Figure 5-1](#) along with the setup for benchmarking the performance. In this setup, a Newport URS50BCC rotation stage rotates the Eshifter stick, while a python program collects the Newport angle and the TMAG5170D magnetic flux measurements and angle calculations. After the data is collected, the first angle collected from the TMAG5170D is compared against the first angle reported by the newport and the difference between these two values is subtracted from all subsequent calculated angles from the TMAG5170D for a 1 point calibration. Subsequently the difference between newport and the shifted TMAG5170D angles is calculated to determine the 1 point calibration angle error in degrees as shown in [Figure 5-2](#).

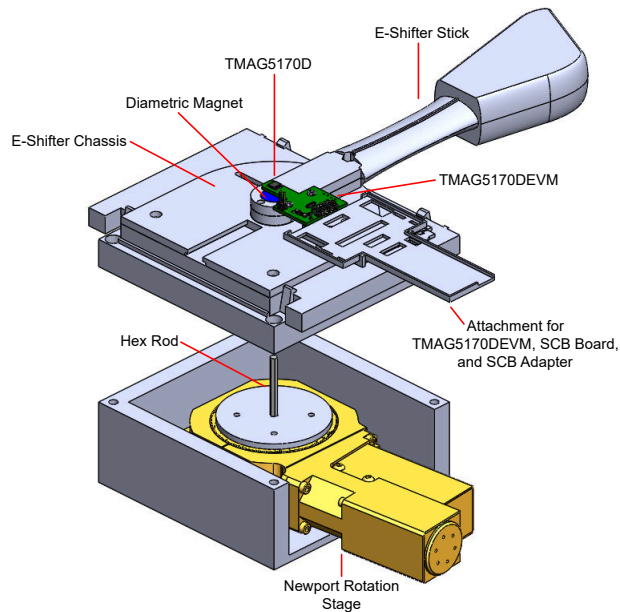


Figure 5-1. Test Setup Exploded View

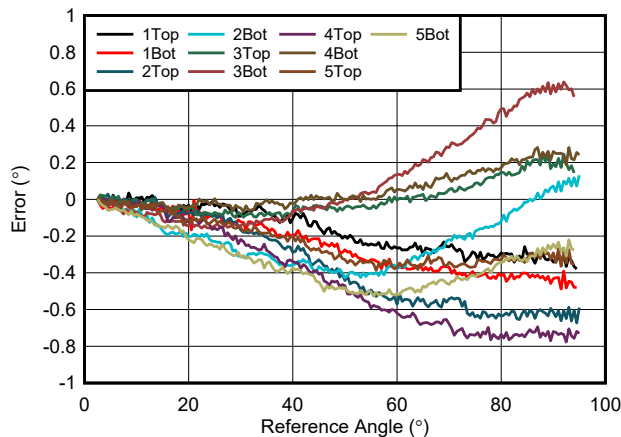


Figure 5-2. 1 pt calibration

Through plotting the 1 point calibrated data versus the newport's angle, which is treated as the absolute angle point of reference, the data in [Figure 5-3](#) appears to be linear and similar to the reference yet does not have

an exact 1 to 1 relationship as shown in Figure 5-2. To minimize the difference between the absolute angle source and the angle procured from the TMAG5170D, a two or more point calibration can be done. For this demo, the movement bounds were used for the two point calibration. The difference between the bound points where then used to determine the coefficients for the equation describing error versus angle calculated from the TMAG5170D as indicated in Figure 5-4.

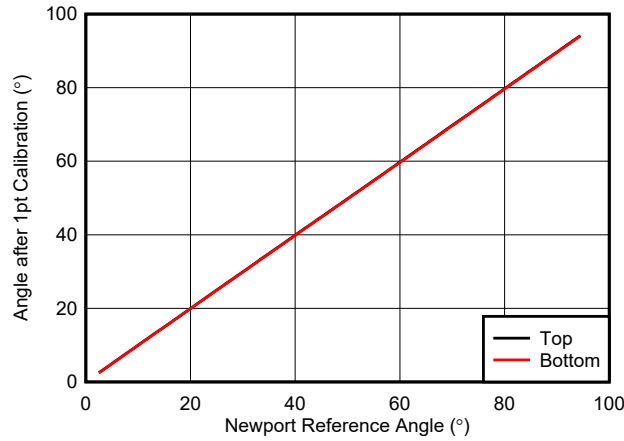
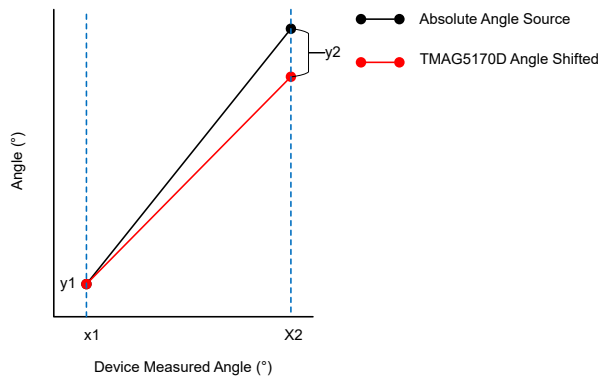


Figure 5-3. Angle Comparison



$$y = mx + b \tag{1}$$

$$y = \text{error} \tag{2}$$

$$x = 1 \text{ pt calibrated TMAG5170 data} \tag{3}$$

$$m = \frac{y_2 - y_1}{x_2 - x_1} \tag{4}$$

$$b = y_2 - mx_2 \tag{5}$$

$$\text{Angle}_{\text{Cal}} = \text{Angle}_{\text{TMAG}} + (m \times \text{Angle}_{\text{TMAG}} + b) \tag{6}$$

Figure 5-4. 2 Point Calibration Method

From the two point calibration, Figure 5-5 was obtained. These results show the max error being between -0.5° and 0.12° as opposed to the previous error bounded between -0.8° and 0.63° . This shows that the max error can be calibrated to be as low as $\pm 0.5^\circ$ and the spread of error reduced by nearly 60%. Extending the calibration to 3 pt, Figure 5-6 was obtained. These errors for this set are -0.15° to 0.14° , providing 80% reduction in the error spread from a single point calibration.

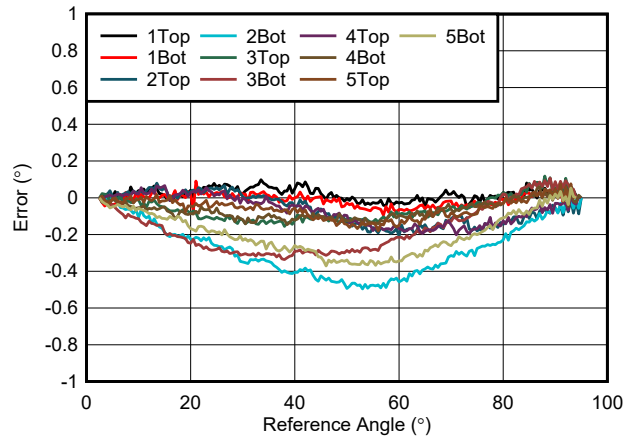


Figure 5-5. 2 pt calibration

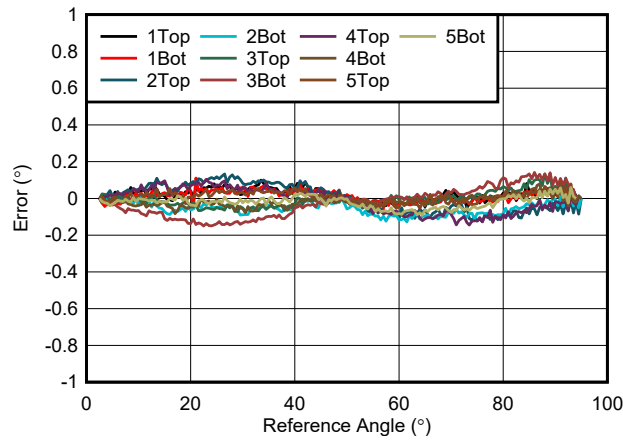


Figure 5-6. 3 pt calibration

As E-shifters need to be redundant, error between sensors is also a very important metric. Figure 5-7 through Figure 5-10 show how many degrees of difference were observed between the sensors on each device. Inspection reveals that no calibration had error bounded to roughly ± 0.6 degrees while 1 point calibration offset the error range from -1.2 to 0.2. This makes sense from the standpoint that both sensors start angle are zeroed in the 1 pt calibration. Calibrations involving more points that compensate for the error exhibit smaller ranges of error with each added calibration point.

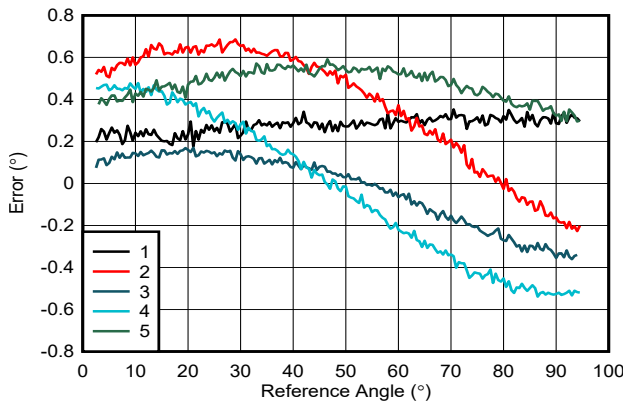


Figure 5-7. No Calibration Error Between Sensor

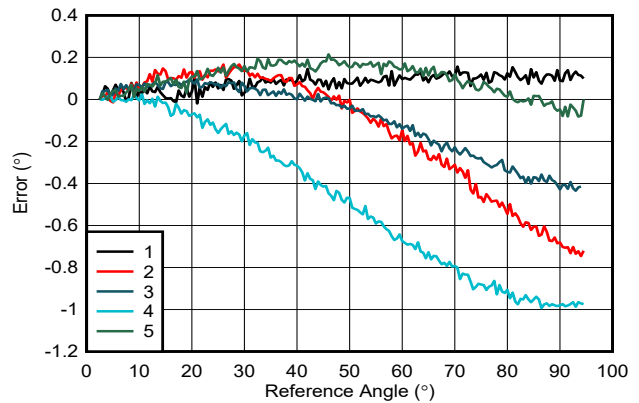


Figure 5-8. 1 pt Calibration Error Between Sensors

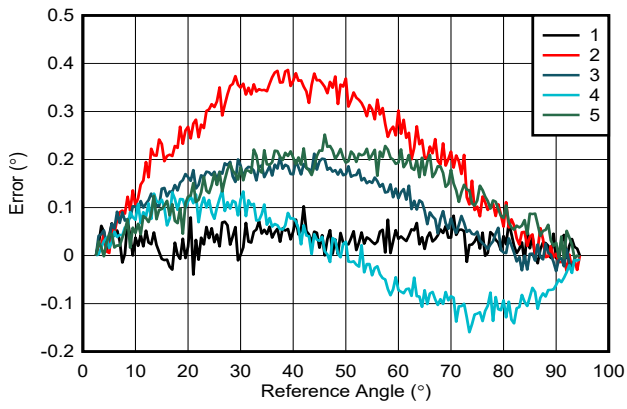


Figure 5-9. 2 pt Calibration Error Between Sensors

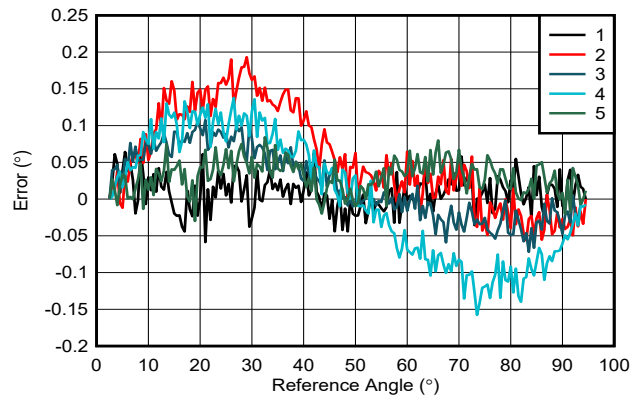


Figure 5-10. 3 pt Calibration Error Between Sensors

6 Error Sources

There are several possible sources of error, many of which correspond to fabrication and assembly. In the process of evaluating on the bench, such error sources are easier to identify, thereby making bench testing a good and necessary practice to embrace before proceeding to mass production. The following list shows all possible error sources identified for this particular design including the ones accounted for in the preliminary design:

- Magnet Offset from the axis of rotation (eccentricity)
- Magnet Tilt
- Sensor Offset
- Sensor Tilt
- Magnet Variation
- Device Variation
- External fields
- Nearby Material Influence
- Bench Setup Error
- Post Processing Error

For an in depth review on how magnet offset and sensor offset impact design, see the [Comparison Between Stacked Die and Side-by-side Die Implementations in Dual-die Magnetic Position Sensors](#) application note.

Bench setup error corresponds to how accurate the reference angle source presumed to be perfect is as well as how precise the device under test (DUT) signal can be measured at the position of interest. For an example of bench setup errors, [Figure 6-1](#) shows how data was initially collected for assessing the design presented in this application note. The measurement errors introduced by the preliminary setup were from the limits of human optical resolution, ability to maintain precise position, and time syncing averaged data. The setup shown in [Figure 5-1](#), removed these sources of error.

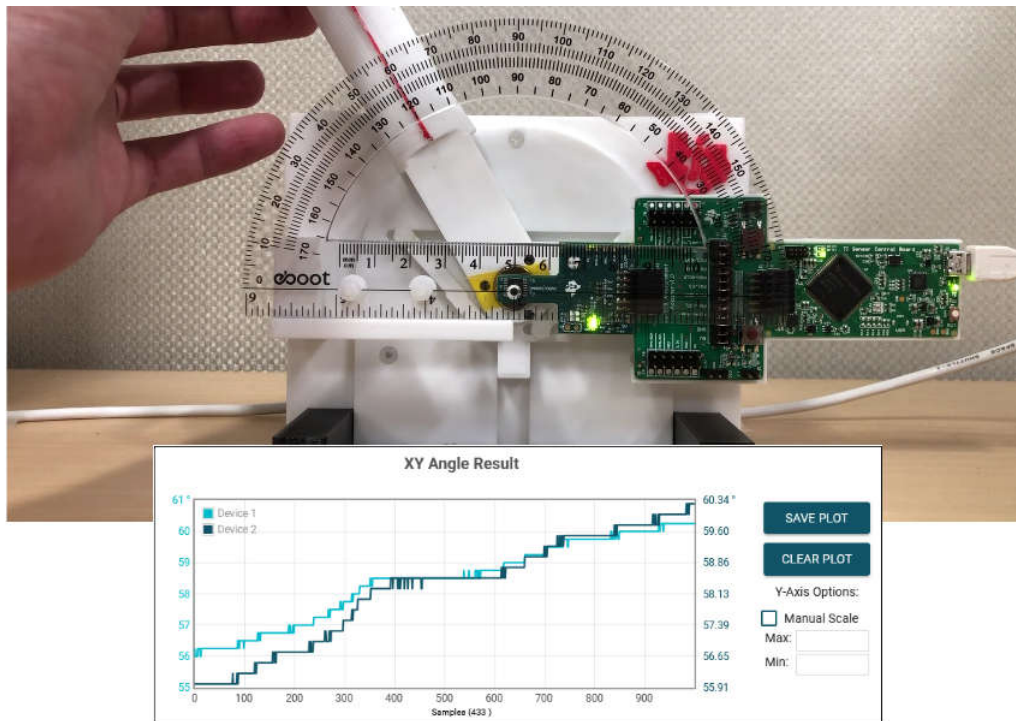


Figure 6-1. preliminary test setup

Post processing errors can stem from how data is averaged, how data is converted from one scale to another, and how calibration algorithms are executed. An example of a post-processing error is shown in [Figure 6-2](#). In this particular case, multiple measurements were made at each discrete step taken during the bench test to account for noise. These measured values which are in twos complement format were then erroneously

averaged like non-two-complement numbers. As a negative number near 0 in twos complement has the same binary format as a large non-two-complement number, when averaged like a non-two-complement number, the averaged value becomes very large for a value that is supposed to be near 0 in standard non-two-complement form.

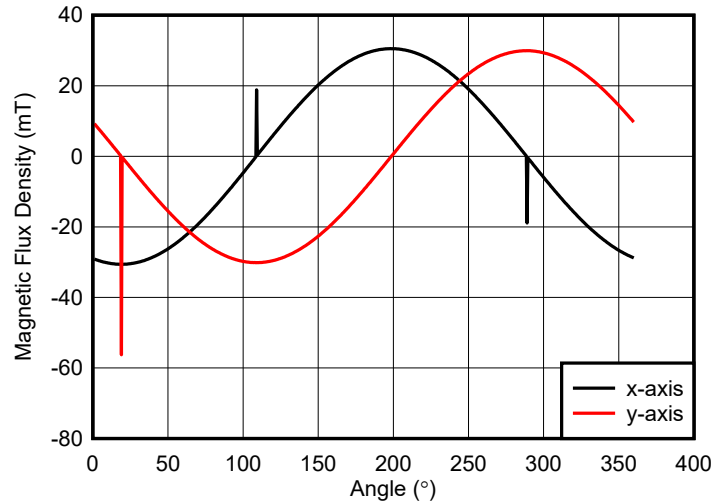


Figure 6-2. Error from User Incorrectly Post Processing

7 Summary

In this application note an E-shifter design is presented. The design flow begins with determining the general method of translating end user position selection into an electrical stimulus that shifter system can process. Then proceeds with showing what Hall-effect devices can be suitable and how to size and space the corresponding magnet accordingly. Results from the featured design indicate what kind of performance was attainable along with a possible calibration method for further improving the accuracy of the design. As any fabricated design has some margin of error introduced in assembly, sources of error were presented to alert designers of various challenges. Despite those challenges, this design achieved absolute angle errors and redundancy errors below $\pm 0.2^\circ$.

8 References

- Texas Instruments, [TMAG5170D-Q1 Dual-Die High-Precision 3D Linear Hall-Effect Sensor With SPI](#) data sheet.
- Texas Instruments, [Comparison Between Stacked Die and Side-by-side Die Implementations in Dual-die Magnetic Position Sensors](#) application note.

IMPORTANT NOTICE AND DISCLAIMER

TI PROVIDES TECHNICAL AND RELIABILITY DATA (INCLUDING DATA SHEETS), DESIGN RESOURCES (INCLUDING REFERENCE DESIGNS), APPLICATION OR OTHER DESIGN ADVICE, WEB TOOLS, SAFETY INFORMATION, AND OTHER RESOURCES "AS IS" AND WITH ALL FAULTS, AND DISCLAIMS ALL WARRANTIES, EXPRESS AND IMPLIED, INCLUDING WITHOUT LIMITATION ANY IMPLIED WARRANTIES OF MERCHANTABILITY, FITNESS FOR A PARTICULAR PURPOSE OR NON-INFRINGEMENT OF THIRD PARTY INTELLECTUAL PROPERTY RIGHTS.

These resources are intended for skilled developers designing with TI products. You are solely responsible for (1) selecting the appropriate TI products for your application, (2) designing, validating and testing your application, and (3) ensuring your application meets applicable standards, and any other safety, security, regulatory or other requirements.

These resources are subject to change without notice. TI grants you permission to use these resources only for development of an application that uses the TI products described in the resource. Other reproduction and display of these resources is prohibited. No license is granted to any other TI intellectual property right or to any third party intellectual property right. TI disclaims responsibility for, and you will fully indemnify TI and its representatives against, any claims, damages, costs, losses, and liabilities arising out of your use of these resources.

TI's products are provided subject to [TI's Terms of Sale](#) or other applicable terms available either on [ti.com](https://www.ti.com) or provided in conjunction with such TI products. TI's provision of these resources does not expand or otherwise alter TI's applicable warranties or warranty disclaimers for TI products.

TI objects to and rejects any additional or different terms you may have proposed.

Mailing Address: Texas Instruments, Post Office Box 655303, Dallas, Texas 75265
Copyright © 2024, Texas Instruments Incorporated